Accepted Article

DR JI HUANG (Orcid ID : 0000-0002-9057-4299)

Article type : Original Article

ORIGINAL ARTICLE

The Phosphoproteomic and Interactomic Landscape of qGL3/OsPPKL1 Mediated Brassinosteroid Signaling in Rice

Xiuying Gao[1,2,4], Jiaqi Zhang[1,2,4], Jianbo Li[1,2], Yuji Wang[1,2], Rong Zhang[1,2], Huaying Du[1,2], Jing Yin[1,2], Guang Cai[1,2], Ruqin Wang[1,2], Baoyi Zhang[1,2], Zhuang Zhao[1,2], Hongsheng Zhang[1,2], Ji Huang[1,2,3,5]

[1] State Key Laboratory of Crop Genetics and Germplasm Enhancement, College of Agriculture, Nanjing Agricultural University, Nanjing 210095, China

[2] Jiangsu Provincial Engineering Research Center of Seed Industry Science and Technology, Nanjing 210095, China

[3] Jiangsu Key Laboratory for Information Agriculture, Nanjing 210095, China

[4] These authors contributed equally to this work.

[5] Address correspondence to huangji@njau.edu.cn

Running title: qGL3-dependent Networks in Rice

SUMMARY

Rice (*Oryza sativa* L.) is one of the most important crops in the world, and grain size is a major component determining rice yield. Recent studies identified a number of grain size regulators, which are involved in the phytohormone signaling, G protein signaling, mitogen-activated protein kinase signaling pathway, ubiquitin-proteasome pathway, or transcriptional regulation. In previous study, we cloned *qGL3*/*OsPPKL1* encoding a

This article has been accepted for publication and undergone full peer review but has not been through the copyediting, typesetting, pagination and proofreading process, which may lead to differences between this version and the Version of Record. Please cite this article as doi: 10.1111/TPJ.15613

This article is protected by copyright. All rights reserved

rice protein phosphatase that negatively modulates brassinosteroid (BR) signaling and grain length. Here, to further explore qGL3-mediated BR signaling network, we performed phosphoproteomic screenings using two pairs of rice materials: the *indica* rice cultivar 9311 and its near-isogenic line NIL^{qgl3} and the *japonica* rice cultivar Dongjin and its *qGL3* knockout mutant *m-qgl3*. Together with qGL3-interacting proteins, we constructed the qGL3-mediated network, which reveals the relationships between BR signaling and other critical signaling pathways. Transgenic plants of these network components showed BR-related alterations in plant architecture. From this network, we validated a qGL3-interacting protein, *O. sativa* VERNALIZATION INSENSITIVE3-LIKE1 (OsVIL1), and demonstrated that qGL3 dephosphorylates OsVIL1 to modulate BR signaling. The qGL3-dependent network uncovered in this study increases our understanding of BR signaling and provides a profound foundation for addressing how BR modulates plant architecture in rice.

KEYWORDS: *Oryza sativa*, grain size, brassinosteroid, qGL3, network

SIGNIFICANT STATEMENT: To enrich the rice brassinosteroid (BR) signaling pathway, the qGL3-dependent network was constructed with phosphoproteomic and interactomic data.

INTRODUCTION

Rice (*Oryza sativa* L.) is an important cereal crop worldwide and is also the primary food source for half of the population in the world. The grain yield of rice is mainly determined by number of panicles per plant, number of grains per panicle, and grain weight. Therefore, grain size, which is positively associated with grain weight, is an important trait for improving yield in rice. The genetic and molecular mechanisms that determine grain size are involved in the mitogen-activated protein kinase (MAPK) signaling pathway, the phytohormone signaling, the ubiquitin-proteasome pathway, G protein signaling, and transcriptional factors (Fan and Li 2019, Li *et al.* 2018, Xu *et al.* 2019).

MAPK cascades transmit developmental or exogenous signals to target proteins through sequential phosphorylation and include three kinases at least: MAPK kinase kinase (MKKK), MAPK kinase (MKK), and MAPK. MKKK receives signal from receptor to activate MKK, and then activates MAPK (Zhang *et al.* 2018). Different combinations of these kinases influence distinct biological processes, including immune response, stomatal patterning, and grain size regulation (Zhang *et al.* 2018). Loss function of *OsMKK4*, *OsMAPK6*, or *OsMKKK10*

This article is protected by copyright. All rights reserved

showed a semi-dwarf phenotype and small grains. *GRAIN SIZE AND NUMBER1* (*GSN1*) encoding a phosphatase that interacts with and inactivates OsMPK6 by dephosphorylation to coordinate the trade-off between grain size and grain number. Interestingly, knocking out *OsMKK4* or *OsMAPK6* resulted in decreased sensitivity to BRs and reduced expression of several BR-related genes (Duan *et al.* 2014, Guo *et al.* 2018, Liu *et al.* 2015, Xu *et al.* 2018). WRKY-type transcription factor WRKY53 is a phosphorylation substrate for the kinases GSK2 and MAPK6, which transduces signals from both BR signaling and the MAPK pathway (Tian *et al.* 2021).

The ubiquitin-proteasome pathway also plays important roles in grain size regulation. *GRAIN WIDTH2* (*GW2*) encodes a RING-type E3 ubiquitin ligase. The *GW2* allele in WY3 (large grain), harboring a 1-bp deletion in the coding region of *GW2*, increases grain size (Song *et al.* 2007). The E3 ubiquitin ligase DA2, which is the homologue of GW2, can ubiquitylate the ubiquitin-receptor DA1 to control grain size (Dong *et al.* 2017, Li *et al.* 2008, Xia *et al.* 2013). The deubiquitination enzyme OsOTUB1 involves both grain width, grain thickness, and grain number mainly by influencing cell expansion. OsOTUB1 could interact with IDEAL PLANT ARCHITECTURE (IPA1), an important regulator of rice architecture, and promote proteasome degradation of OsSPL14 (Wang *et al.* 2017).

Phytohormone, such as brassinosteroids (BRs), cytokinin, auxin, and gibberellins (GAs), plays important roles in plant development (Li *et al.* 2018). BRs are a group of growth-promoting steroid hormones regulating plant architecture, which is an important trait to determine grain yield (Nolan *et al.* 2020). For example, loss of function of receptor kinase *O. sativa* BRASSINOSTEROID INSENSITIVE1 (OsBRI1) (Nakamura *et al.* 2006) or its partner *O. sativa* BRI1-ASSOCIATED RECEPTOR KINASE1 (OsBAK1) (Li *et al.* 2009) results in BR insensitive phenotypes and small grains. The downstream components of BR signaling, such as *O. sativa* GLYCOGEN SYNTHASE KINASES (OsGSK1, OsGSK2, and OsGSK3) (Gao *et al.* 2019, Koh *et al.* 2007, Tong *et al.* 2012), also affect grain size, and overexpressing *O. sativa* BRASSINAZOLE-RESISTANT1 (OsBZR1) (Bai *et al.* 2007) forms larger grain length, grain width, and grain weight. Auxin has also been demonstrated to play important roles determining grain size. *THOUSAND GRAIN WEIGHT6* (*TGW6*) encodes IAA glucose hydrolase, which involves early endosperm development by regulating IAA supply. The Kasalath (light grain) *TGW6* allele increases the accumulation of carbohydrates without change in grain quality (Ishimaru *et al.* 2013). The relationships between auxin and BR signaling pathway have been analyzed, for instance, auxin and BR coordinately function to increase lateral root development, lamina joint bending, and hypocotyl elongation. These effects of auxin and BRs on various events suggested the interdependency of their signaling. The expression of auxin-related genes, such as *INDOLE-3-ACETIC*

This article is protected by copyright. All rights reserved

Accepted Article

ACID3 (*IAA3*), *IAA5*, *DR5* promoter (a synthetic auxin-responsive cis-acting element), and *SAUR-AC1* is induced by brassinolide (BL) (Goda *et al.* 2004, Nemhauser *et al.* 2004). Moreover, SMALL ORGAN SIZE1 (SMOS1) affects organ size through mediating auxin signaling, and its interacting protein SMOS2, a GRAS protein, DWARF AND LOW-TILLERING (DLT), which was demonstrated to be involved in BR signaling. The interaction between these SMOS proteins could be a critical point for BR and auxin signaling (Hirano *et al.* 2017). Recent findings suggest that cytokinin plays important roles in controlling grain size. A grain number QTL, *Gn1a*, encodes a cytokinin oxidase (OsCKX2), which modulates cytokinin accumulation. Reduced expression of *OsCKX2* promotes cytokinin accumulation in inflorescence meristems and increases grain number and yield (Ashikari *et al.* 2005). An abiotic stress induced gene, *O. sativa STRESS TOLERANCE AND GRAIN LENGTH* (*OsSGL*), is involved in stress tolerance and grain length regulation. Loss function of *OsSGL* alters the expression of several CK-related genes, suggesting that OsSGL may influence stress response and grain length through modulating cytokinin signal transduction (Wang *et al.* 2016).

The mechanism of transcriptional regulatory factors regulating grain size have been widely analyzed. For example, GRAIN LENGTH AND WEIGHT7 (GLW7) (Si *et al.* 2016), GRAIN WIDTH8 (GW8) (Wang *et al.* 2015a, Wang *et al.* 2012, Wang *et al.* 2015b, Zhou *et al.* 2015), GRAIN LENGTH7 (GL7) (Wang *et al.* 2015a, Wang *et al.* 2015b, Zhou *et al.* 2015), GRAIN SIZE2 (GS2) (Che *et al.* 2016, Duan *et al.* 2016, Hu *et al.* 2015, Li *et al.* 2016, Sun *et al.* 2016), and GRAIN LENGTH4 (GL4) (Wu *et al.* 2017). G protein signaling is involved in a variety of developmental processes in rice and plays an important role determining grain size. *GRAIN SIZE3* (*GS3*), encoding a Gγ protein, which is one of the major QTLs for grain size (Mao *et al.* 2010, Sun *et al.* 2018). DENSE AND ERECT PANICLE1 (DEP1) is also a Gγ protein and plays an important role in grain number regulation in rice (Botella 2012, Huang *et al.* 2009, Sun *et al.* 2014). In addition to Gγ subunits, a Gα subunit (RGA1) (Ashikari *et al.* 1999, Fujisawa *et al.* 1999, Oki *et al.* 2009) and a Gβ subunit (RGB1) (Liu *et al.* 2018a, Utsunomiya *et al.* 2011) have been identified: loss function of *RGA1* or *RGB1* resulted in small and round grains and overexpression of *RGB1* also reduced grain size. The genetic analyses were performed to elucidate the relationship between G proteins. Moreover, OsMADS1, a grain length regulator, was reported to be a downstream effector of G protein signaling and directly interacted with GS3 and DEP1 (Liu *et al.* 2018a, Yu *et al.* 2018).

In previous studies, we cloned a major quantitative trait locus (QTL), *qGL3*, which negatively regulates grain length and BR signaling in rice. N411 is a rice variety with a rare *qgl3* allele, that produces longer grain phenotype,

This article is protected by copyright. All rights reserved

Accepted Article

and 9311 is another variety with relatively smaller grains. *qGL3*, encodes a protein phosphatase with two Kelch-like domains (OsPPKL1), which is the homologue of BSU1. The qGL3 protein in N411 has two amino acids substitution compared with qGL3 in 9311, which influenced the dephosphorylation activity of qGL3, as the activity of $qGL3^{N411}$ was lower than $qGL3^{9311}$. We also found that BL significantly increased the lamina joint bending of *m-qgl3* (*qGL3* knocking out mutant) and NIL^{qgl3} (carrying the $qGL3^{N411}$ allele in 9311) indicating the negative role of qGL3 is abolished in N411 and then induced BR signaling. The qGL3-mediated BR signaling model illustrates that qGL3 dephosphorylates and stabilizes OsGSK3, an essential negative regulator of BR signaling, resulting the decreased protein level and cytoplasmic localization of OsBZR1. In the current study, we performed a large-scale phosphoproteomic analysis to map the qGL3-dependent network in two groups of rice materials, ensuring the accuracy of the identification of qGL3-related proteins. As a complementary method, we identified qGL3-interacting proteins by yeast two-hybrid screening of a library constructed from young panicle tissues. The interactomic data revealed potential direct substrates of qGL3. Integration of the two data sets elucidated plant-specific links offering a rich resource to address fundamental questions about how qGL3 affects rice architecture and investigates the molecular mechanisms underlying BR signaling in rice. The phosphoproteomic and interactomic analysis uncovered complex networks between BR signaling and other pathways with qGL3 as the link. This network lays the foundation for addressing how the BR signal is transduced and modulates plant architecture in rice.

RESULTS

Phosphoproteomic and Interactomic Screening Reveal qGL3/OsPPKL1-dependent Components in Rice

We previously showed that loss-of-function of *qGL3* displayed enhanced BR signaling phenotypes, including increased lamina joint bending and longer grains. Treatment with brassinolide (BL), a highly active BR, significantly increased lamina joint bending and coleoptile length in *qGL3* mutant *m-qgl3* and the near-isogenic line NIL^{qgl3} (carrying the $qGL3^{N411}$ allele in the 9311 background), implying that the negative role is abolished in N411 and the BR signaling is therefore induced and grain length increased (Gao *et al.* 2019). In the current study, to better understand phosphorylation events and identify differential phosphorylation sites affected by qGL3/OsPPKL1, we performed phosphoproteomic screening using *m-qgl3*, NIL^{qgl3}, and their corresponding wild-type lines (Figure 1a). We used iTRAQ LC-MS/MS to detect phosphorylated proteins in these lines. The proteins were extracted and digested

This article is protected by copyright. All rights reserved

Accepted Article

from each sample with trypsin/Lys-C, enriched the phosphopeptides using TiO_2 magnetic beads, and the enriched phosphopeptides were analyzed by iTRAQ labeling quantitative MS (Figure 1a).

To obtain a bioinformatic overview of the subcellular localizations of the phosphorylated proteins identified in our phosphoproteome, we performed gene ontology (GO) analysis of proteins in the cellular component category. Analysis of the distribution patterns in the phosphoproteome showed that 46%, 31%, and 9% of the proteins were located in the nucleus, plasma membrane, and cytoplasm, respectively. By contrast, proteins in the remaining compartments such as the chloroplast, vacuole, Golgi, and mitochondria accounted for less than 5% of total proteins (Figure 1b). A filtered data set of 3106 phosphopeptides on 1477 proteins were collected for further analyses. In total, the phosphorylation status of 212 and 200 proteins was altered in *m-qgl3* and *NIL^{qgl3}*, respectively, while the phosphorylation of 80 proteins (~40% of the total phosphorylated proteins altered in either line) was commonly regulated in both materials (Figure 1c, Figure 2, and Table S1).

Identifying motifs around phosphosites provides valuable information about the substrate specificities of the phosphatase. Motif enrichment analysis showed that several motifs were over-represented among the phosphopeptides. The main motifs appear to be conserved among qGL3 phosphatase targets are: motif 1: R-X-X-S-SP; motif 2: SP-X-X-SP; motif 3: S-X-X-X-SP-X-R (Figure S1). To validate the protein level and status of differentially expressed phosphorylated proteins, we performed western-blot analysis for selected differentially expressed phosphorylated proteins in wild type and qGL3-related plants, including OsMKKK65 and OsGF14e (Figure 2). The slower migrating bands correspond to the phosphorylated form of OsMKKK65 and OsGF14e. All these two proteins showed similar phosphorylation tendencies as the phosphoproteomic data indicated (Figure 1d). Moreover, the absence of the slower-migrating bands following treatment with calf intestine alkaline phosphatase (CIP) confirmed their identity as phosphorylated proteins (Figure 1e).

Although our phosphoproteomic data analysis provided a view of qGL3-dependent phosphoproteins, but it could not discriminate between direct and indirect substrates of qGL3. To extend our analysis of the qGL3-dependent network, we investigated the qGL3-interacting proteins via yeast two-hybrid screening analysis using qGL3 as bait. We choose several qGL3-interacting proteins (GIPs) for further analysis to verify the reliability of the interactomic data, including *O. sativa* VERNALIZATION INSENSITIVE3-LIKE1 (OsVIL1), *O. sativa* MAPK4 (OsMPK4), *O. sativa* CYTOCHROME C LIKE (OsCCL), *O. sativa* RNA-binding KH domain-containing protein RCF3 (OsRCF3), *O. sativa* CALCIUM-DEPENDENT PTOTEIN KINASE24 (OsCPK24), *O. sativa* JASMONATE ZIM-DOMAIN

This article is protected by copyright. All rights reserved

PROTEIN6 (OsJAZ6), and *O. sativa* UBIQUITIN CONJUGATING ENZYME15 (OsUBC15) (Table S2). The yeast two hybrid assay was employed to analyze the interaction between qGL3 and GIPs. The results showed that qGL3 could interact with these proteins in yeast cells (Figure 3). Next, bimolecular fluorescence complementation (BiFC) assays were performed to test in vivo interaction of qGL3 with GIPs. *N. benthamiana* epidermal cells expressing qGL3-nYFP and GIPs-cYFP showed strong fluorescence signals (Figure 4). Confocal microscopic analyses of the transformed tobacco leaves revealed that qGL3 interacted with OsCPK24 in cytoplasm, and the YFP signal was observed in the nucleus when tobacco cells co-expressed qGL3-YN and OsVIL1/OsRCF3/OsJAZ6-YC. In BiFC with qGL3 and OsMPK4/OsCCL/OsUBC15, the YFP signal was observed in both cytoplasm and nucleus (Figure 4).

Modulation of OsVIL1 by qGL3 Involves BR Signaling

In qGL3-dependent network, we chose OsVIL1 for further analysis. We have demonstrated the interactions between qGL3 and OsVIL1 via the yeast two-hybrid and BiFC assays *in vivo*. To confirm the interaction between qGL3 and OsVIL1 *in vitro*, we performed GST pull-down assays to analyze the interaction. In this assay, GST fused OsVIL1 pulled down His-qGL3, whereas GST alone could not pull down His-qGL3 (Figure 5a). We then performed dephosphorylation assay to determine whether qGL3 could directly dephosphorylate OsVIL1 *in vitro*. The activated GST-OsVIL1 reacted with His-qGL3 and then we detected the phosphorylation status of OsVIL1 using a phos-tag assay in which phosphorylated proteins are visualized on the nitrocellulose membrane. It was found that the GST-OsVIL1 band incubated with His-qGL3 was fainter than the control band (Figure 5b). Next we measured the effects of BL treatment on the expression levels of *OsVIL1*. *OsVIL1* substantially increased in WT plants treated with BL (Figure 5c). Moreover, the relative expression level of *OsVIL1* decreased in *m-qgl3* compared with WT (Figure 5d). These results suggest that qGL3 dephosphorylates OsVIL1 to modulate BR signaling in rice.

Mutations of qGL3-dependent components alter plant architecture

BRs play essential roles in regulating plant growth and development, including plant height, tiller number, and grain size, highlighting the potential for targeting BR signaling to improve rice productivity. To explore whether the newly discovered qGL3-related proteins are involved in regulating plant architecture and BR signaling, we selected some differentially expressed phosphoproteins from phosphoproteome and qGL3-interacting proteins from Y2H screening for further research, and obtained their T-DNA insertion mutants.

This article is protected by copyright. All rights reserved

Accepted Article

From these mutants, 7 were chosen for rice architecture analysis (Figure 6 and Figure S2a). The mutants were divided into the two types based on phenotypes: type I: mutants with BR signaling-enhanced phenotypes, such as *osmkkk65*, *osz3*, and *osc3h23*; type II: mutants with BR signaling-suppressed phenotypes, such as *osvil1*, *oszar1*, *ossus1*, and *osbak10* (Figure 6a-6d). These T-DNA insertion mutants were confirmed by co-segregation test of the T-DNA insertion with the mutant phenotype. As shown in Figure S2b, a combination of PCR results of primer set LP/RP + LB/RB enable us to easily determine the genotype of plants in the T-DNA insertion.

Considering that some of the mutants showed the classic phenotype of mutants with enhanced or blocked BR signaling, we hypothesized that some of the mutants might be involved in modulating BR signaling. Therefore, we examined the BL sensitivity of the wild types and mutants. Coleoptile is a specialized tissue that is very sensitive to BL. Exogenous BL could effectively increase coleoptile elongation. We found that BL significantly promoted the coleoptile length in *osmkkk65* and *osbak10* mutants, and decreased the coleoptile length in *osvil1*, *osz3*, *oszar1*, and *ossus1* mutants. Next, the effects of BL treatment on root inhibition were examined. The results showed that BL treatment inhibited root elongation in *osc3h23*, *osmkkk65*, and *osbak10* plants, while *osz3*, *oszar1*, and *ossus1* seedlings showed insensitive to BL treatment compared with wild types (Figure 6e-6g). Interestingly, the relatively increased coleoptile length of *osc3h23* seedlings and reduced root length of *osvil1* seedlings showed no obvious change compared with WT (Figure 6e-6g).

Then, we measured the expression levels of BR biosynthetic genes and BR signaling related genes, including *OsD2*, *OsDWF4*, *OsDWF*, *OsBZR1*, *OsGSK2*, and *OsGSK3*, in the wild types and T-DNA mutants using quantitative real-time PCR (RT-qPCR) and found that these genes were differentially expressed in these mutants compared with the wild type (Figure S3). In *osc3h23* mutant: the transcript levels of *OsBZR1* increased and the expression level of *OsD2* and *OsGSK3* decreased in these two mutants compared with wild type. In *osmkkk65* mutant: the transcript levels of both *OsD2*, *OsDWF4*, *OsDWF*, *OsGSK2*, and *OsGSK3* decreased, and the expression level of *OsBZR1* increased. In *osz3* mutant: all of these genes showed no obvious change in expression level excluding *OsDWF4* and *OsDWF*. In *oszar1* and *osbak10* mutants: the expression level of these genes showed opposite tendency compared with *osmkkk65* mutant. In *ossus1* mutant: the expression level of OsBZR1 decreased and the levels of both OsDWF4, OsGSK2, and OsGSK3 increased, indicating that the BR signaling might be repressed in *ossus1* mutant (Figure S3).

To investigate the effect of natural variation in these selected proteins on grain length, plant height, and panicle number, the sequences of accessions of cultivated rice from the 3000 Rice Genome Project were analyzed. Three

This article is protected by copyright. All rights reserved

Accepted Article

haplotypes were identified at *OsFCA* locus, and Hap3 forms shorter grains compared to Hap1 and Hap2 (Figure S4). Interestingly, the panicle number showed no obvious change between these three haplotypes. These results suggest that the locus may play a role in grain size, plant height, and panicle number regulation at the species level (Figure S4).

Construction of qGL3-dependent network

To construct the qGL3-dependent network, we combined the phosphoproteomic and interactomic data for the analyses. From interactomic data, it was identified 67 protein–protein interactions in yeast cells, including interactions with OsGSKs, OsJAZ6, OsCPK20, and OsMPK4. Using String and Cytoscape visualization, we constructed protein–protein interaction networks with qGL3-related differentially expressed phosphorylated proteins and qGL3-interacting proteins (Figure S5). Based on this network, several proteins share complex relationships with multiple proteins, including Os01g47750 (Similar to U2 snRNP auxiliary factor), Os03g17710 (RS2Z subfamily protein 38), Os02g147800 (a splicing factor), Os01g26940 (a transposon protein), Os05g36120 (a polypyrimidine tract-binding protein), Os08g37960 (an RNA recognition motif-containing protein), and Os05g01540 (serine/arginine repetitive matrix protein 1) (Figure S5). This analyses reveal the close relationship between qGL3-related phosphorylated proteins and qGL3-interacting proteins.

The complete list of interactions and annotations can be used to build networks with Cytoscape and to extract relevant information about qGL3-dependent networks and subnetworks reported in the present study in rice. The networks combining qGL3-interacting proteins and phosphoproteomic data comprised 113 proteins. This phosphoproteomic and interactomic data contain proteins involved in the cell cycle, 14-3-3 homologs, proteins involved in mRNA splicing and processing, transcriptional regulation, the protein degradation pathway, and hormonal pathways including BR, cytokinin, auxin, ethylene, and jasmonic acid signaling pathways (Figure 7). Overall, this integrated network sheds light on the various processes that are modulated by qGL3 in rice.

Currently available evidence suggests that grain size is modulated by multiple signaling pathways including phytohormone, ubiquitin-proteasomal degradation, mitogen-activated protein kinase (MAPK) signaling, and G-protein signaling pathways. In the qGL3-dependent network, OsCPK20/24 (involved in the cytokinin pathway), OsGSK1/2/3 (involved in BR signaling), and OsIAA3/21 (involved in auxin signaling), have tight relationships with qGL3. The cell wall and cell cycle regulation are also responsible for grain length. The proteins affected by qGL3

This article is protected by copyright. All rights reserved

include CESA4/7/8/9, which function in both cell wall and cell cycle pathways. MAPK cascades are evolutionarily conserved signaling modules in eukaryotes and play critical roles in defense signals and transducing developmental signals in plants. MAPK cascades are also involved in grain size. In the qGL3-related network, we found OsMPK4 interacted with qGL3 suggesting a possible link between BR signaling and the MAPK pathways. The ubiquitin proteasome pathway plays important roles in seed size. OsUBC15 and eight other proteins were classified into the proteasome degradation pathway (Figure 7).

Further analysis of this network might uncover unexplored functions of qGL3, providing ideas and methods for elucidating the BR signaling pathway and the regulation of grain length. This network adds an extra layer to the complex relationship between BR signaling and qGL3, revealing an interaction of the qGL3 complex with BR response factors. In addition to uncovering downstream signaling events mapped by phosphoproteomic screening, the interactomic data may shed light on upstream regulatory mechanisms.

DISCUSSION

Studies have shown that qGL3 protein is an essential component of the BR signaling pathway, and negatively regulates grain length and BR signaling by both dephosphorylating and blocking degradation of OsGSK3 kinase (Gao *et al.* 2019). Here, to enrich qGL3-dependent network in rice, we combined a phosphoproteomic screen and interactomic screen to identify both upstream and downstream network components.

From the phosphoproteomic data, a number of proteins including kinases, transcriptional factors, and enzymes were identified. Phosphopeptides were enriched from protein extracts using LC-MS/MS. 3160 phosphopeptides and number of phosphorylation sites were identified. Identifying motifs around phosphosites provides valuable information about the substrate specificities of the phosphatase. Motif enrichment analysis showed that several motifs were over-represented among the phosphopeptides. The main motifs appear to be conserved among qGL3 phosphatase targets are: motif 1: R-X-X-S-SP; motif 2: SP-X-X-SP; motif 3: S-X-X-X-SP-X-R. In animals, the majority of known GSK3-like kinases substrates contain a typical phosphorylation motif: S/T-X-X-X-S/T (X is any amino acid). In Arabidopsis, BZR1/BES1 have 25 putative GSK3 phosphorylation motifs, and several of these amino acids were experimentally confirmed as in vitro or in vivo phosphorylation sites (Gampala *et al.* 2007, Ryu *et al.* 2010, Ryu *et al.* 2007, Tang *et al.* 2008). Similarly, mass spectrometry analysis indicated that Ser^{230} and Thr^{234} of MKK4 are the essential AtBIN2 phosphorylation sites (Khan *et al.* 2013). In our previous study, qGL3 could

This article is protected by copyright. All rights reserved

phosphorylate OsGSK3 and the phosphorylated OsGSK3 degraded by 26S proteasome pathway. Since the qGL3 protein is a phosphatase, the 48 differentially up-regulated proteins may include qGL3 substrates and the 32 down-regulated proteins may include OsGSK3 substrates. According to the enrich motif analysis from qGL3-related phosphoproteomic data, it was found that some up-regulated proteins contains the dephosphorylation amino acid sites recognized by qGL3, such as Os05g50830, Os11g29380, OsTRX9. In the down-regulated phosphorylated proteins, OsCESA9, OsSUS1, OsCESA8, and rnaBP1 include the OsGSK3 phosphorylation motifs. Interestingly, the peptides phosphorylated by SnRK2.10 has revealed that its phosphorylation site is L-X-R-X-X-S, and OsSUS1 contains this motif, indicating that OsSUS1 might also be phosphorylated by SnRK2.10 kinase. Collectively, the phsophoproteomic data could identify the phosphorylation sites of proteins affected by qGL3, however, qGL3 may not directly bind to these proteins. The interactomic data could identify proteins physically interacting with qGL3, but whether this interaction is related to phosphorylation modification remains unknown. In total, the interactomic and phosphoproteomic analysis complemented each other to describe the qGL3 regulatory network in rice.

Grain size, plant height and tiller number are important agronomical traits involved in BR signaling in rice. Taking grain size as an example, recent studies have shown that rice grain size was determined by multiple signaling pathways, including auxin, cytokinin, G protein signaling, MAPK signaling, ubiquitin-proteasome pathway, and transcriptional regulations (Fan and Li 2019, Li *et al.* 2018). By exploring the qGL3-mediated networks in this study, we revealed the qGL3-mediated networks between BR signaling and other pathways including auxin, cytokinin, MAPK and proteasome pathways, suggesting that qGL3 is a critical node bridging BR and other signaling pathways in the regulation of rice growth and development (Figure S6).

Relationships among plant hormones or other signaling pathway play important roles in modulating plant growth and tolerance to various environmental conditions. The qGL3-dependent network combined qGL3-interacting proteins and our phosphorylation data. The network adds an extra layer to the complex relationship between BR signaling and the other essential signaling pathway regulating plant architecture. Interactions of BR signaling with other phytohormone signaling pathways regulate plant yields and stress responses, such as BR and GA biosynthesis and signaling processes interact each other to form a complex network that affects plant height in rice. The interaction between BR and auxin signaling pathways is mediated by LPA1 and OsEMF1. An *OsEMF1* knockout mutant exhibited reduced plant height, leaf angle, and grain size and was insensitive to BR. Finally, OsARF11 directly interacts with OsEMF1 to enhance the expression of OsBRI1 (Liu *et al.* 2018b).

This article is protected by copyright. All rights reserved

To shed light on the discovered qGL3-related proteins, we highlighted several proteins in this work. These include flowering pathway (OsVIL1 and OsFCA), MAPK signaling related proteins (OsMKKK65 and OsMPK4), ubiquitin-proteasome related protein (OsUBC15), auxin signaling related proteins (OsGSK5), cytokinin signaling related protein (OsCPK24), BR signaling related proteins (OsBAK10, OsZAR1, OsSUS1, and OsZ3), transcriptional regulation proteins (OsRCF3 and OsC3H23).

The flowering time is determined by genetic components and various environmental factors, including temperature, stress, and day length. The crops can be managed to increase productivity through flowering time control under environmental challenges (Izawa 2021). The RNA-binding protein FCA in Arabidopsis plays important roles in flowering pathway, which promotes flowering by suppressing FLOWERING LOCUS C (FLC) (Feng *et al.* 2011). Notably, studies demonstrate that FCA incorporates temperature signal with flowering pathway and participate in plant response to temperature changes (Lee *et al.* 2014). In this research, the phsophorylated protein level of OsFCA increased in both *m-qgl3* mutant and NIL^{qgl3} plants compared with wild types. The vernalization pathway is well known to involved in predicting seasonal changes. Previous studies of VIN3-like (VIL) proteins focused on their roles in vernalization. VIL1 is involved in vernalization and photoperiod pathways, indicting the critical roles of VIL proteins in flowering pathway. A rice homolog of Arabidopsis VIN3, *LC2*, is one of the key regulator in controlling rice flowering time. It has also been found that the expression of LC2 is induced by BR (Zhao *et al.* 2010). Therefore, further studies would be expected to elucidate how OsFCA and OsVIL1 involve flowering time and grain length through modulating BR signaling, which was mediated by qGL3 in rice.

The MAPK cascades are conserved signaling modules and play critical roles in plant development. Loss function of *OsMKKK10* produces small and light grains, and studies determined that OsMPK6 also positively affects grain length (Xu *et al.* 2018). OsMPK6 directly interacts with and phosphorylates the transcription factor DST to enhance its transcriptional activation of OsCKX2, indicating that the OsMKKK10-OsMKK4-OsMPK6 pathway regulates panicle by modulating cytokinin pathway. Recent studies demonstrate that BR signaling and MAPK pathway coordinately regulate rice architecture and grain size. OsGSK2, which is a key regulator in rice BR signaling, phosphorylates OsMAPKK4 to suppress OsMAPK6 activity, indicating that GSK2 might also modulate MAPK pathway (Tian *et al.* 2021). In our research, qGL3 directly interacts with OsMPK4 and indirectly regulates the phosphorylation of OsMKKK65. It would be worthwhile to analyze the relationship between BR signaling and MAPK pathway mediated by qGL3 in the future study.

This article is protected by copyright. All rights reserved

Plant development and defense response are coordinately regulated by phytohormones, including BR and jasmonic acid (JA), which are growth-promoting and defense-related hormones, respectively. In rice lamina joint inclination regulation, BR and JA play antagonistic role. JASMONATE ZIM-DOMAIN (JAZ) proteins are the key suppressors in JA signaling, which bind to and inhibit transcription factors to promote JA-responsive genes expression. Studies demonstrates that blocking GSK3-like kinase activity can reduce JA signaling in rice, indicating its essential role as a link between BR and JA signaling. As a key regulator of BR signaling, OsGSK2 interacts with and phosphorylates and promotes the degradation of OsJAZ4, suggested that OsJAZ4-mediated BR sensitivity might be dependent on OsGSK2. The interaction between OsJAZ4 and OsGSK2 reveals a relationship between JA and BR signaling (He *et al.* 2020). In this research, we found that qGL3 could interact with OsJAZ6 in yeast cells and tobacco epidermal cells. We hypothesize that qGL3 may dephosphorylate OsJAZ6 to regulate their protein level and then modulate JA signaling. Our research might provide insight into the interacting mechanism between BR and JA signaling.

Moreover, as qGL3 interacts with OsCPK24 and OsGSK5, therefore, BR signaling mediated by qGL3 might also modulate cytokinin and auxin signaling in grain length regulation. Furthermore, several transcriptional regulators were identified in qGL3-dependent network, including OsRCF3 from interactomic data and OsC3H23 from phosphoproteomic data. In rice, BR functions in coordination with other signaling pathways in regulating various processes of plant development. Plenty of studies revealed that BR plays an extensive role in regulating grain size. Our research aimed to analyze the interactions between BR signaling and the other signaling pathway via clarifying the molecular mechanisms of qGL3 and its dependent components. Overall, the qGL3-dependent network constructing with phosphoproteomic and interactomic data sheds light on the rice architecture regulation and highlight unexplored factors of BR signaling in rice.

METHODS

Plant materials

Rice (*Oryza sativa*) varieties 9311 (*xian*/*indica*), Dongjin (DJ, *geng*/*japonica*), and Hwayoung (HY, *geng*/*japonica*) were used as the wild types. The T-DNA insertion mutants in the DJ and HY backgrounds were obtained from Kyung Hee University, Korea (http://cbi.khu.ac.kr/RISD_DB.html). NIL^{qgl3} was developed in the genetic background of *indica* variety 9311 and the *qgl3* allele is in the *japonica* N411 background. The agronomic traits of the plants were

This article is protected by copyright. All rights reserved

examined in plants grown in the field in Nanjing, China under natural growth conditions. To evaluate tiller number and plant height, 10 plants were examined before harvesting. For each line, the lengths of 15 filled grains were measured with an electronic digital caliper (WSEEN, Hangzhou, China).

Phosphopeptide preparation

Total protein extraction and digestion were performed as described previously (Hou *et al.* 2015). For phosphopeptide enrichment, 100 μg peptide mixture of each sample was labeled using iTRAQ reagent according to the manufacturer's instructions (Applied Biosystems). The labeled peptides were mixed, concentrated by a vacuum concentrator and resuspended in 500 μL 1×DHB buffer (0.0025g DHB [12617, Sigma], 13.3% Acetonitrile [I592230123, Merck], 0.017% Trifluoroacetic Acid [T6508, Sigma]). Then, TiO2 beads were added and agitated for 2 hours. The centrifugation was carried out for 1 min at 5000 g, resulting the beads. And washed with 50 μL of washing buffer I (30% Acetonitrile, 1% Trifluoroacetic Acid) three times and then 50 μL of washing buffer II (80% Acetonitrile, 0.1% Trifluoroacetic Acid) three times to remove the remaining non-adsorbed material. Finally, the phosphopeptides were eluted with 50 μL of elution buffer (40% Acetonitrile, 15% $NH_3 \cdot H_2O$) three times, followed by lyophilization and MS analysis (Bioprofile Technology CO., LTD, Shanghai, China).

LC-MS/MS

LC-MS/MS analysis was performed on a Q Exactive mass spectrometer (Thermo Scientific) that was coupled to Easy nLC (Thermo Fisher Scientific) for 240 min. The mass spectrometer was operated in positive ion mode. MS data was acquired using a data-dependent top10 method dynamically choosing the most abundant precursor ions from the survey scan (300–1800 m/z) for HCD fragmentation. Automatic gain control (AGC) target was set to $3e^6$, and maximum inject time to 10 ms. Dynamic exclusion duration was 40.0 s. Survey scans were acquired at a resolution of 70,000 at 200 m/z and resolution for HCD spectra was set to 17,500 at 200 m/z, and isolation width was 2 m/z. Normalized collision energy was 30 eV and the underfill ratio, which specifies the minimum percentage of the target value likely to be reached at maximum fill time, was defined as 0.1%. The instrument was run with peptide recognition mode enabled.

Motif discovery

For identification of over-represented motifs among the qGL3-related phosphopeptides, the sequence (−7, +7) around

This article is protected by copyright. All rights reserved

Accepted Article

the identified qGL3-dependent sites was analyzed with the Motif-X algorithm at a significance level of 1.80×10^{-4} (Schwartz and Gygi 2005).

Network analysis and visualization

For interaction analysis of the qGL3-dependent phosphorylation network and protein interactome, the sequences of the corresponding genes were loaded into String 11.0 (Search Tool for the Retrieval of Interacting Genes/Proteins) and Cytoscape (version 3.7.2).

Genotyping of T-DNA insertion mutant plants

Polymerase chain reaction (PCR) genotyping of the T-DNA insertion mutants was performed by using the following primers: LP, RP and LB/RB, which are listed in Table S3. PCR was conducted with an initial step of 95°C incubation for 5 min, followed by 30 cycles of 95°C for 15 s, 55°C for 15 s, and 72°C for 2 min; with a final extension at 72°C for 5 min.

BL treatment

The wild types and T-DNA insertion mutants were grown in the field or greenhouse under a 30°C/25°C day/night cycle. BL (Sigma, USA) was dissolved in DMSO to suitable concentrations as stock solutions. For the coleoptile growth and root inhibition experiments, 30 rice seeds were grown on 0.3% agar medium with or without BL at 30°C under continuous darkness for 5 days.

Yeast two-hybrid assays

For the yeast two-hybrid assays, *qGL3* was cloned into the pGBKT7 vector, and *GIPs* were cloned into the pGADT7 vector, resulting in qGL3-BD and GIPs-AD, respectively. The reporter gene assay was performed following the manufacturer's instructions (Clontech, USA). The yeast cells were cultured on SD/-W-L and SD/-W-L-H-A medium containing X-α-gal at 30°C for 3 days in the dark. SD/-W-L is yeast culture medium without tryptophan and leucine. SD/-W-L-H-A is culture medium without tryptophan, leucine, histidine, and adenine. The PCR primers used for the yeast two-hybrid assays are listed in Table S3.

BiFC

For BiFC analysis, *qGL3* was cloned into the pSPYNE173 vector, and *GIPs* were cloned into the pSPYCE (M) vector.

This article is protected by copyright. All rights reserved

The plasmids were transformed into *Agrobacterium tumefaciens* strain EHA105. *A. tumefaciens* cells containing each construct were prepared and mixed to an OD_{600} of 0.5:0.5. YFP fluorescence was visualized under a confocal laser-scanning microscope at 40–48 h after infiltration. The PCR primers used for the BiFC assays are listed in Table S3.

GST pull-down assay and *in vitro* dephosphatase assay

To test the interaction between qGL3 and OsVIL1, the coding sequence of *qGL3* was cloned into the pET-30a vector to produce the His-qGL3 fusion proteins. The coding sequence of *OsVIL1* was cloned into the pGEX-2T vector to produce the GST-OsVIL1 fusion proteins. For pull-down, 0.5 μg GST-OsVIL1 or GST was incubated with GST Bind Resin (70541, Novagen, USA) for 2 hours at 4°C then 0.5 μg His-qGL3 was added. The incubation continued for 2 hours and then washed three times. The beads were boiled in 1× SDS loading buffer and separated by 10% SDS-PAGE. The His antibody (9991S, Cell signaling technology, USA) and GST antibody (2624S, Cell signaling technology, USA) were used to detect the proteins.

For *in vitro* dephosphatase assay, the phosphorylated GST-OsVIL1 was obtained when it was expressed in the *Escherichia coli* strain BL21 during cell culture, and then it was purified with GST Bind Resin. To dephosphorylate protein GST-OsVIL1, His-qGL3 was mixed with the phosphorylated GST-OsVIL1 protein and incubated for 2 hours at 30°C. Samples were separated by 10% SDS-PAGE followed by immunoblotting with biotin-pendant Zn^{2+}-Phos-tag (BTL-111) according to the manufacturer's instructions (Western Blot Analysis of Phosphorylated Proteins-Chemiluminescent Detection using Biotinylated Phos-tag, Wako, Nard Institute, Ltd, Japan).

ACCESSION NUMBERS

Sequence data from this article can be found in the GenBank/EMBL databases under the following accession numbers: *qGL3*, Os03g44500; *OsGSK3*, Os02g14130; *OsBZR1*, Os07g39220; *OsGSK2*, Os05g11730; *OsD2*, Os01g10040; *OsDWF4*, Os03g12660; *OsDWF*, Os03g40540; *OsVIL1*, Os08g12430; *OsMPK4*, Os10g38950; *OsCCL*, Os01g66180; *OsRCF3*, Os01g13470; *OsCPK24*, Os11g07040; *OsJAZ6*, Os03g28940; *OsUBC15*, Os02g16040; *OsMKKK65*, Os07g43900; *OsZ3*, Os03g05390; *OsZAR1*, Os11g19480; *OsC3H23*, Os03g21160; *OsSUS1*, Os03g28330; and *OsBAK10*, Os03g16010. The phosphoproteomics data have been deposited to the ProteomeXchange Consortium via the PRIDE partner Repository with the dataset identifier PXD025494.

This article is protected by copyright. All rights reserved

Accepted Article

ACKNOWLEDGEMENTS

We would like to thank the support of Center for Bioinformatics, Nanjing Agricultural University, and Rui Wang for the omics analysis. This work was supported by Natural Science Foundation of China (32071918, 32000227), Youth Science Foundation of Jiangsu Province (SBK2019040714), the Fundamental Research Funds for the Central Universities (JCQY201901, KJQN202102), Jiangsu Collaborative Innovation Center for Modern Crop Production and Cyrus Tang Seed Innovation Center, Nanjing Agricultural University.

DATA AVAILABILITY STATEMENT

All relevant data can be found within the manuscript and its supporting materials.

AUTHOR CONTRIBUTIONS

J.H. and X.G. conceived the original research plans, performed bioinformatics analysis, and wrote the manuscript; X.G. was involved in all stages of experimental work and data analysis; J.Z., J.L., Y.W., R.Z., H.D., J.Y., G.C., R.-Q.W., B.Z., and Z.Z. helped to perform experiments; J.H. and H.Z. supervised the project.

CONFLICT OF INTEREST

The authors have no conflicts of interest to declare.

SUPPORTING INFORMATION

Figure S1. De novo motif analysis of the qGL3-related phosphosites.

Figure S2. Molecular characterization of the mutants.

Figure S3. Expression patterns of BR biosynthesis and signaling-related genes in the seedlings of the WT and T-DNA insertion mutant plants. The transcript level of the WT was defined as "1". Data are means ± $_{SE}$ (n = 3). Statistical analyses were performed by Duncan's multiple range tests. The presence of the same lowercase letter denotes a non-significant difference for expression levels of *OsBZR1*, *OsD2*, *OsDWF4*, *OsGSK2*, *OsGSK3*, or *OsDWF*, respectively, between wild types and T-DNA insertion mutants ($P > 0.05$).

Figure S4. Natural variations of the differentially phosphorylated protein genes and the effects on grain length, plant height, and panicle number.

Figure S5. The network of the qGL3-related differentially phosphorylated proteins and qGL3-interacting proteins

This article is protected by copyright. All rights reserved

Accepted Article

constructed with String and Cytoscape.

Figure S6. qGL3-mediated relationships between BR signaling and other pathways. Proteins highlighted in blue were from interactomic data, and proteins highlighted in black were from phosphoproteomic data.

Table S1. qGL3-dependent phosphoproteomic data.

Table S2. qGL3-related interactomic data.

Table S3. Primers used in this study.

REFERENCES

Ashikari, M., Wu, J.Z., Yano, M., Sasaki, T., and Yoshimura, A. (1999). Rice gibberellin-insensitive dwarf mutant gene Dwarf 1 encodes the alpha-subunit of GTP-binding protein. P Natl Acad Sci USA **96,** 10284-10289.

Ashikari, M., Sakakibara, H., Lin, S., Yamamoto, T., Takashi, T., Nishimura, A., Angeles, E.R., Qian, Q., Kitano, H., and Matsuoka, M. (2005). Cytokinin oxidase regulates rice grain production. Science **309,** 741-745.

Bai, M.Y., Zhang, L.Y., Gampala, S.S., Zhu, S.W., Song, W.Y., Chong, K., and Wang, Z.Y. (2007). Functions of OsBZR1 and 14-3-3 proteins in brassinosteroid signaling in rice. P Natl Acad Sci USA **104,** 13839-13844.

Botella, J.R. (2012). Can heterotrimeric G proteins help to feed the world? Trends Plant Sci **17,** 563-568.

Che, R.H., Tong, H.N., Shi, B.H., Liu, Y.Q., Fang, S.R., Liu, D.P., Xiao, Y.H., Hu, B., Liu, L.C., Wang, H.R., Zhao, M.F., and Chu, C.C. (2016). Control of grain size and rice yield by GL2-mediated brassinosteroid responses. Nat Plants **2**.

Dong, H., Dumenil, J., Lu, F.H., Na, L., Vanhaeren, H., Naumann, C., Klecker, M., Prior, R., Smith, C., McKenzie, N., Saalbach, G., Chen, L.L., Xia, T., Gonzalez, N., Seguela, M., Inze, D., Dissmeyer, N., Li, Y.H., and Bevan, M.W. (2017). Ubiquitylation activates a peptidase that promotes cleavage and destabilization of its activating E3 ligases and diverse growth regulatory proteins to limit cell proliferation in Arabidopsis. Gene Dev **31,** 197-208.

Duan, P.G., Rao, Y.C., Zeng, D.L., Yang, Y.L., Xu, R., Zhang, B.L., Dong, G.J., Qian, Q., and Li, Y.H. (2014). SMALL GRAIN 1, which encodes a mitogen-activated protein kinase kinase 4, influences grain size in rice. Plant J **77,** 547-557.

Duan, P.G., Ni, S., Wang, J.M., Zhang, B.L., Xu, R., Wang, Y.X., Chen, H.Q., Zhu, X.D., and Li, Y.H. (2016).

This article is protected by copyright. All rights reserved

Regulation of OsGRF4 by OsmiR396 controls grain size and yield in rice. Nat Plants **2**.

Fan, Y.W., and Li, Y.B. (2019). Molecular, cellular and Yin-Yang regulation of grain size and number in rice. Mol Breeding **39**.

Feng, W., Jacob, Y., Veley, K.M., Ding, L., Yu, X., Choe, G., and Michaels, S.D. (2011). Hypomorphic alleles reveal FCA-independent roles for FY in the regulation of FLOWERING LOCUS C. Plant Physiol **155,** 1425-1434.

Fujisawa, Y., Kato, T., Ohki, S., Ishikawa, A., Kitano, H., Sasaki, T., Asahi, T., and Iwasaki, Y. (1999). Suppression of the heterotrimeric G protein causes abnormal morphology, including dwarfism, in rice. P Natl Acad Sci USA **96,** 7575-7580.

Gampala, S.S., Kim, T.W., He, J.X., Tang, W., Deng, Z., Bai, M.Y., Guan, S., Lalonde, S., Sun, Y., Gendron, J.M., Chen, H., Shibagaki, N., Ferl, R.J., Ehrhardt, D., Chong, K., Burlingame, A.L. and Wang, Z.Y. (2007) An essential role for 14-3-3 proteins in brassinosteroid signal transduction in Arabidopsis. Dev Cell, **13**, 177-189.

Gao, X.Y., Zhang, J.Q., Zhang, X.J., Zhou, J., Jiang, Z.S., Huang, P., Tang, Z.B., Bao, Y.M., Cheng, J.P., Tang, H.J., Zhang, W.H., Zhang, H.S., and Huang, J. (2019). Rice qGL3/OsPPKL1 Functions with the GSK3/SHAGGY-Like Kinase OsGSK3 to Modulate Brassinosteroid Signaling. Plant Cell **31,** 1077-1093.

Goda, H., Shimada, Y., Fujioka, S., and Yoshida, S. (2004). Classification of brassinosteroid-regulated genes based on expression profiles in bri1 and in response to a protein kinase inhibitor, staurosporin. Biosci Biotech Bioch **68,** 1605-1607.

Guo, T., Chen, K., Dong, N.Q., Shi, C.L., Ye, W.W., Gao, J.P., Shan, J.X., and Lin, H.X. (2018). GRAIN SIZE AND NUMBER1 Negatively Regulates the OsMKKK10-OsMKK4-OsMPK6 Cascade to Coordinate the Trade-off between Grain Number per Panicle and Grain Size in Rice. Plant Cell **30,** 871-888.

He, Y.Q., Hong, G.J., Zhang, H.H., Tan, X.X., Li, L.L., Kong, Y.Z., Sang, T., Xie, K.L., Wei, J., Li, J.M., Yan, F., Wang, P.C., Tong, H.N., Chu, C.C., Chen, J.P., and Sun, Z.T. (2020). The OsGSK2 Kinase Integrates Brassinosteroid and Jasmonic Acid Signaling by Interacting with OsJAZ4. Plant Cell **32,** 2806-2822.

Hirano, K., Yoshida, H., Aya, K., Kawamura, M., Hayashi, M., Hobo, T., Sato-Izawa, K., Kitano, H., Ueguchi-Tanaka, M., and Matsuoka, M. (2017). SMALL ORGAN SIZE 1 and SMALL ORGAN SIZE 2/DWARF AND LOW-TILLERING Form a Complex to Integrate Auxin and Brassinosteroid Signaling in

This article is protected by copyright. All rights reserved

Accepted Article

Rice. Mol Plant **10,** 590-604.

Hou, Y.X., Qiu, J.H., Tong, X.H., Wei, X.J., Nallamilli, B.R., Wu, W.H., Huang, S.W., and Zhang, J. (2015). A comprehensive quantitative phosphoproteome analysis of rice in response to bacterial blight. BMC Plant Biol **15**.

Hu, J., Wang, Y.X., Fang, Y.X., Zeng, L.J., Xu, J., Yu, H.P., Shi, Z.Y., Pan, J.J., Zhang, D., Kang, S.J., Zhu, L., Dong, G.J., Guo, L.B., Zeng, D.L., Zhang, G.H., Xie, L.H., Xiong, G.S., Li, J.Y., and Qian, Q. (2015). A Rare Allele of *GS2* Enhances Grain Size and Grain Yield in Rice. Mol Plant **8,** 1455-1465.

Huang, X.Z., Qian, Q., Liu, Z.B., Sun, H.Y., He, S.Y., Luo, D., Xia, G.M., Chu, C.C., Li, J.Y., and Fu, X.D. (2009). Natural variation at the *DEP1* locus enhances grain yield in rice. Nat Genet **41,** 494-497.

Ishimaru, K., Hirotsu, N., Madoka, Y., Murakami, N., Hara, N., Onodera, H., Kashiwagi, T., Ujiie, K., Shimizu, B., Onishi, A., Miyagawa, H., and Katoh, E. (2013). Loss of function of the IAA-glucose hydrolase gene *TGW6* enhances rice grain weight and increases yield. Nat Genet **45,** 707-713.

Izawa, T. (2021) What is going on with the hormonal control of flowering in plants? Plant J, **105**, 431-445.

Khan, M., Rozhon, W., Bigeard, J., Pflieger, D., Husar, S., Pitzschke, A., Teige, M., Jonak, C., Hirt, H. and Poppenberger, B. (2013) Brassinosteroid-regulated GSK3/Shaggy-like kinases phosphorylate mitogen-activated protein (MAP) kinase kinases, which control stomata development in Arabidopsis thaliana. J Biol Chem, **288**, 7519-7527.

Koh, S., Lee, S.C., Kim, M.K., Koh, J.H., Lee, S., An, G., Choe, S., and Kim, S.R. (2007). T-DNA tagged knockout mutation of rice *OsGSK1*, an orthologue of Arabidopsis BIN2, with enhanced tolerance to various abiotic stresses. Plant Mol Biol **65,** 453-466.

Lee, H.J., Jung, J.H., Cortes Llorca, L., Kim, S.G., Lee, S., Baldwin, I.T., and Park, C.M. (2014). FCA mediates thermal adaptation of stem growth by attenuating auxin action in Arabidopsis. Nat Commun **5,** 5473.

Li, D., Wang, L., Wang, M., Xu, Y.Y., Luo, W., Liu, Y.J., Xu, Z.H., Li, J., and Chong, K. (2009). Engineering *OsBAK1* gene as a molecular tool to improve rice architecture for high yield. Plant Biotechnol J **7,** 791-806.

Li, N., Xu, R., Duan, P., and Li, Y. (2018). Control of grain size in rice. Plant Reprod **31,** 237-251.

Li, S.C., Gao, F.Y., Xie, K.L., Zeng, X.H., Cao, Y., Zeng, J., He, Z.S., Ren, Y., Li, W.B., Deng, Q.M., Wang, S.Q., Zheng, A.P., Zhu, J., Liu, H.N., Wang, L.X., and Li, P. (2016). The OsmiR396c-OsGRF4-OsGIF1 regulatory module determines grain size and yield in rice. Plant Biotechnol J **14,** 2134-2146.

This article is protected by copyright. All rights reserved

Li, Y.H., Zheng, L.Y., Corke, F., Smith, C., and Bevan, M.W. (2008). Control of final seed and organ size by the DA1 gene family in Arabidopsis thaliana. Gene Dev **22,** 1331-1336.

Liu, Q., Han, R.X., Wu, K., Zhang, J.Q., Ye, Y.F., Wang, S.S., Chen, J.F., Pan, Y.J., Li, Q., Xu, X.P., Zhou, J.W., Tao, D.Y., Wu, Y.J., and Fu, X.D. (2018a). G-protein beta gamma subunits determine grain size through interaction with MADS-domain transcription factors in rice. Nat Commun **9**.

Liu, S.Y., Hua, L., Dong, S.J., Chen, H.Q., Zhu, X.D., Jiang, J.E., Zhang, F., Li, Y.H., Fang, X.H., and Chen, F. (2015). OsMAPK6, a mitogen-activated protein kinase, influences rice grain size and biomass production. Plant J **84,** 672-681.

Liu, X., Yang, C.Y., Miao, R., Zhou, C.L., Cao, P.H., Lan, J., Zhu, X.J., Mou, C.L., Huang, Y.S., Liu, S.J., Tian, Y.L., Nguyen, T.L., Jiang, L., and Wan, J.M. (2018b). DS1/OsEMF1 interacts with OsARF11 to control rice architecture by regulation of brassinosteroid signaling. Rice (N Y) **11,** 46.

Mao, H.L., Sun, S.Y., Yao, J.L., Wang, C.R., Yu, S.B., Xu, C.G., Li, X.H., and Zhang, Q.F. (2010). Linking differential domain functions of the GS3 protein to natural variation of grain size in rice. P Natl Acad Sci USA **107,** 19579-19584.

Nakamura, A., Fujioka, S., Sunohara, H., Kamiya, N., Hong, Z., Inukai, Y., Miura, K., Takatsuto, S., Yoshida, S., Ueguchi-Tanaka, M., Hasegawa, Y., Kitano, H., and Matsuoka, M. (2006). The role of *OsBRI1* and its homologous genes, *OsBRL1* and *OsBRL3*, in rice. Plant Physiol **140,** 580-590.

Nemhauser, J.L., Mockler, T.C., and Chory, J. (2004). Interdependency of brassinosteroid and auxin signaling in Arabidopsis. Plos Biol **2,** 1460-1471.

Nolan, T.M., Vukasinovic, N., Liu, D., Russinova, E., and Yin, Y. (2020). Brassinosteroids: Multidimensional Regulators of Plant Growth, Development, and Stress Responses. Plant Cell **32,** 295-318.

Oki, K., Inaba, N., Kitagawa, K., Fujioka, S., Kitano, H., Fujisawa, Y., Kato, H., and Iwasaki, Y. (2009). Function of the alpha Subunit of Rice Heterotrimeric G Protein in Brassinosteroid Signaling. Plant Cell Physiol **50,** 161-172.

Ryu, H., Cho, H., Kim, K. and Hwang, I. (2010) Phosphorylation dependent nucleocytoplasmic shuttling of BES1 is a key regulatory event in brassinosteroid signaling. Mol Cells, **29**, 283-290.

Ryu, H., Kim, K., Cho, H., Park, J., Choe, S. and Hwang, I. (2007) Nucleocytoplasmic shuttling of BZR1 mediated by phosphorylation is essential in Arabidopsis brassinosteroid signaling. Plant Cell **19**, 2749-2762.

This article is protected by copyright. All rights reserved

Schwartz, D. and Gygi, S.P. (2005) An iterative statistical approach to the identification of protein phosphorylation motifs from large-scale data sets. Nat Biotechnol **23**, 1391-1398.

Si, L.Z., Chen, J.Y., Huang, X.H., Gong, H., Luo, J.H., Hou, Q.Q., Zhou, T.Y., Lu, T.T., Zhu, J.J., Shangguan, Y.Y., Chen, E.W., Gong, C.X., Zhao, Q., Jing, Y.F., Zhao, Y., Li, Y., Cui, L.L., Fan, D.L., Lu, Y.Q., Weng, Q.J., Wang, Y.C., Zhan, Q.L., Liu, K.Y., Wei, X.H., An, K., An, G., and Han, B. (2016). OsSPL13 controls grain size in cultivated rice. Nat Genet **48,** 447-457.

Song, X.J., Huang, W., Shi, M., Zhu, M.Z., and Lin, H.X. (2007). A QTL for rice grain width and weight encodes a previously unknown RING-type E3 ubiquitin ligase. Nat Genet **39,** 623-630.

Sun, H.Y., Qian, Q., Wu, K., Luo, J.J., Wang, S.S., Zhang, C.W., Ma, Y.F., Liu, Q., Huang, X.Z., Yuan, Q.B., Han, R.X., Zhao, M., Dong, G.J., Guo, L.B., Zhu, X.D., Gou, Z.H., Wang, W., Wu, Y.J., Lin, H.X., and Fu, X.D. (2014). Heterotrimeric G proteins regulate nitrogen-use efficiency in rice. Nat Genet **46,** 652-656.

Sun, P.Y., Zhang, W.H., Wang, Y.H., He, Q., Shu, F., Liu, H., Wang, J., Wang, J.M., Yuan, L.P., and Deng, H.F. (2016). OsGRF4 controls grain shape, panicle length and seed shattering in rice. Journal of Integrative Plant Biology **58,** 836-847.

Sun, S.Y., Wang, L., Mao, H.L., Shao, L., Li, X.H., Xiao, J.H., Ouyang, Y.D., and Zhang, Q.F. (2018). A G-protein pathway determines grain size in rice. Nat Commun **9**.

Tang, W.Q., Deng, Z.P., Oses-Prieto, J.A., Suzuki, N., Zhu, S.W., Zhang, X., Burlingame, A.L. and Wang, Z.Y. (2008) Proteomics studies of brassinosteroid signal transduction using prefractionation and two-dimensional DIGE. Mol Cell Proteomics **7**, 728-738.

Tian, X., He, M., Mei, E., Zhang, B., Tang, J., Xu, M., Liu, J., Li, X., Wang, Z., Tang, W., Guan, Q., and Bu, Q. (2021). WRKY53 Integrates Classic Brassinosteroid Signaling and the Mitogen-Activated Protein Kinase Pathway to Regulate Rice Architecture and Seed Size. Plant Cell.

Tong, H.N., Liu, L.C., Jin, Y., Du, L., Yin, Y.H., Qian, Q., Zhu, L.H., and Chu, C.C. (2012). DWARF AND LOW-TILLERING Acts as a Direct Downstream Target of a GSK3/SHAGGY-Like Kinase to Mediate Brassinosteroid Responses in Rice. Plant Cell **24,** 2562-2577.

Utsunomiya, Y., Samejima, C., Takayanagi, Y., Izawa, Y., Yoshida, T., Sawada, Y., Fujisawa, Y., Kato, H., and Iwasaki, Y. (2011). Suppression of the rice heterotrimeric G protein beta-subunit gene, *RGB1*, causes dwarfism and browning of internodes and lamina joint regions. Plant J **67,** 907-916.

This article is protected by copyright. All rights reserved

Accepted Article

Accepted Article

Wang, M., Lu, X., Xu, G., Yin, X., Cui, Y., Huang, L., Rocha, P., and Xia, X. (2016). *OsSGL*, a novel pleiotropic stress-related gene enhances grain length and yield in rice. Sci Rep **6,** 38157.

Wang, S.K., Wu, K., Yuan, Q.B., Liu, X.Y., Liu, Z.B., Lin, X.Y., Zeng, R.Z., Zhu, H.T., Dong, G.J., Qian, Q., Zhang, G.Q., and Fu, X.D. (2012). Control of grain size, shape and quality by OsSPL16 in rice. Nat Genet **44,** 950-955.

Wang, S.K., Li, S., Liu, Q., Wu, K., Zhang, J.Q., Wang, S.S., Wang, Y., Chen, X.B., Zhang, Y., Gao, C.X., Wang, F., Huang, H.X., and Fu, X.D. (2015a). The OsSPL16-GW7 regulatory module determines grain shape and simultaneously improves rice yield and grain quality. Nat Genet **47,** 949-955.

Wang, S.S., Wu, K., Qian, Q., Liu, Q., Li, Q., Pan, Y.J., Ye, Y.F., Liu, X.Y., Wang, J., Zhang, J.Q., Li, S., Wu, Y.J., and Fu, X.D. (2017). Non-canonical regulation of SPL transcription factors by a human OTUB1-like deubiquitinase defines a new plant type rice associated with higher grain yield. Cell Res **27,** 1142-1156.

Wang, Y.X., Xiong, G.S., Hu, J., Jiang, L., Yu, H., Xu, J., Fang, Y.X., Zeng, L.J., Xu, E.B., Xu, J., Ye, W.J., Meng, X.B., Liu, R.F., Chen, H.Q., Jing, Y.H., Wang, Y.H., Zhu, X.D., Li, J.Y., and Qian, Q. (2015b). Copy number variation at the *GL7* locus contributes to grain size diversity in rice. Nat Genet **47,** 944-949.

Wu, W.G., Liu, X.Y., Wang, M.H., Meyer, R.S., Luo, X.J., Ndjiondjop, M.N., Tan, L.B., Zhang, J.W., Wu, J.Z., Cai, H.W., Sun, C.Q., Wang, X.K., Wing, R.A., and Zhu, Z.F. (2017). A single-nucleotide polymorphism causes smaller grain size and loss of seed shattering during African rice domestication. Nat Plants **3**.

Xia, T., Li, N., Dumenil, J., Li, J., Kamenski, A., Bevan, M.W., Gao, F., and Li, Y.H. (2013). The Ubiquitin Receptor DA1 Interacts with the E3 Ubiquitin Ligase DA2 to Regulate Seed and Organ Size in Arabidopsis. Plant Cell **25,** 3347-3359.

Xu, R., Li, N., and Li, Y. (2019). Control of grain size by G protein signaling in rice. J Integr Plant Biol **61,** 533-540.

Xu, R., Duan, P.G., Yu, H.Y., Zhou, Z.K., Zhang, B.L., Wang, R.C., Li, J., Zhang, G.Z., Zhuang, S.S., Lyu, J., Li, N., Chai, T.Y., Tian, Z.X., Yao, S.G., and Li, Y.H. (2018). Control of Grain Size and Weight by the OsMKKK10-OsMKK4-OsMAPK6 Signaling Pathway in Rice. Mol Plant **11,** 860-873.

Yu, J., Miao, J., Zhang, Z., Xiong, H., Zhu, X., Sun, X., Pan, Y., Liang, Y., Zhang, Q., Abdul Rehman, R.M., Li, J., Zhang, H., and Li, Z. (2018). Alternative splicing of *OsLG3b* controls grain length and yield in japonica rice. Plant Biotechnol J.

Zhang, M., Su, J., Zhang, Y., Xu, J., and Zhang, S. (2018). Conveying endogenous and exogenous signals: MAPK

This article is protected by copyright. All rights reserved

cascades in plant growth and defense. Curr Opin Plant Biol **45,** 1-10.

Zhao, S.Q., Hu, J., Guo, L.B., Qian, Q. and Xue, H.W. (2010) Rice leaf inclination2, a VIN3-like protein, regulates leaf angle through modulating cell division of the collar. Cell Res, **20**, 935-947.

Zhou, Y., Miao, J., Gu, H.Y., Peng, X.R., Leburu, M., Yuan, F.H., Gu, H.W., Gao, Y., Tao, Y.J., Zhu, J.Y., Gong, Z.Y., Yi, C.D., Gu, M.H., Yang, Z.F., and Liang, G.H. (2015). Natural Variations in *SLG7* Regulate Grain Shape in Rice. Genetics **201,** 1591-1599.

FIGURE LEGENDS

Figure 1. Identification of qGL3-dependent phosphoproteins by quantitative phosphoproteomics.

(a) Schematic representation of the large-scale phosphoscreen individual steps are highlighted and annotated. (b) The subcellular localization of qGL3-dependent phosphoproteins predicted by gene ontology (GO) annotation. (c) The number of identified differentially expressed phosphoproteins shown by Venn diagram in DJ, *m-qgl3*, 9311, and NIL^{qgl3}. (d) The protein level and status of OsMKKK65 and OsGF14e in DJ, *m-qgl3*, 9311, and NIL^{qgl3} plants. For the quantitation of protein level, we first normalized to heat shock protein (HSP), and then analyzed the protein level with the phosphorylated protein level versus the unphosphorylated protein level. The phosphorylated protein level versus the unphosphorylated protein level of DJ or 9311 was defined as 1. (e) Immunoprecipitated OsMKKK65 and OsGF14e proteins from WT was treated with calf intestine alkaline phosphatase (CIP).

Figure 2. The qGL3-related phosphoproteins commonly detected in two pairs of rice materials (*m-qgl3*/DJ) and (NIL^{qgl3}/9311). Hierarchical cluster analysis of the qGL3-dependent phosphosites. For clustering, average estimated phosphosite intensities were normalized per row by median subtraction and colored according to the indicated color gradient. Specific clusters embedding, respectively, upregulated or downregulated phosphopeptides upon (*m-qgl3* vs. DJ) vs. (NIL^{qgl3} vs.9311).

Figure 3. Yeast two-hybrid analysis of qGL3 and its interacting proteins (GIPs). The GIPs were fished from rice young panicle library using qGL3 as bait, including *O. sativa* VERNALIZATION INSENSITIVE3-LIKE1 (OsVIL1), *O. sativa* MAPK4 (OsMPK4), *O. sativa* CYTOCHROME C LIKE (OsCCL), *O. sativa* RNA-binding KH domain-containing protein RCF3 (OsRCF3), *O. sativa* CALCIUM-DEPENDENT PTOTEIN KINASE24 (OsCPK24), *O. sativa* JASMONATE ZIM-DOMAIN PROTEIN6 (OsJAZ6), and *O. sativa* UBIQUITIN CONJUGATING

This article is protected by copyright. All rights reserved

ENZYME15 (OsUBC15).

Figure 4. BiFC analysis of the qGL3 and its interacting proteins. The YFP fluorescence signals and autofluorescence signals from tobacco cells were pseudo-colored as yellow and red, respectively. Scale bars, 20 μm.

Figure 5. qGL3 interacts with and dephosphorylates OsVIL1.

(a) GST pull-down assay of the qGL3 and OsVIL1 interaction. Anti-His antibody was used to detect the output protein. (b) *In vitro* dephosphorylation analysis. Phosphorylation was detected with biotin-pendant Zn^{2+} phos-tag (BTL-111). Coomassie blue staining of the proteins used for the dephosphorylation assay. (c) The relative expression level of *OsVIL1* under BL treatment. The transcript level of the WT was defined as "1". Data are means ± SE (n = 3). The data were compared by Student's *t*-test. ***P < 0.001, **P < 0.01. (d) Expression patterns of *OsVIL1* in the seedlings of the WT and *m-qgl3* plants. The transcript level of the WT was defined as "1". Data are means ± SE (n = 3). The data were compared by Student's *t*-test. ***P < 0.001.

Figure 6. Phenotypes of the mutants of qGL3/OsPPKL1-related proteins.

(a) Morphology of these mutants at the reproductive phase. (b-d) Quantification of grain length (b), plant height (c), and tiller number (d) of these mutants compared with the wild types (Dongjin, DJ; Hwayoung, HY). For quantification of grain length, data are means ± SE (n = 15). For quantification of plant height and tiller number, data are means ± SE (n = 10). The data were compared by Student's *t*-test. ***P < 0.001, **P < 0.01, *P < 0.05, and "ns" means no significance. (e) Coleoptile elongation and root elongation of the wild types and T-DNA insertion mutant plants in response to 1 μM BL. (f) and (g) Quantitative comparison of coleoptile elongation (f) and root inhibition (g) of these plants. Data are means ± SE (n = 15). Statistical analyses were performed by Duncan's multiple range tests. The presence of the same lowercase letter denotes a non-significant difference between wild types and T-DNA insertion mutants under mock or BL treatment, respectively (P > 0.05).

Figure 7. The qGL3-dependent network. For interaction analysis of the qGL3-related phosphorylated proteins and qGL3-interacting proteins, the sequences of the corresponding genes were loaded into String 11.0 (Search Tool for the Retrieval of Interacting Genes/Proteins) (https://string-db.org/) and Cytoscape (version 3.7.2) (http://www.cytoscape.org/).

This article is protected by copyright. All rights reserved

Accepted Article

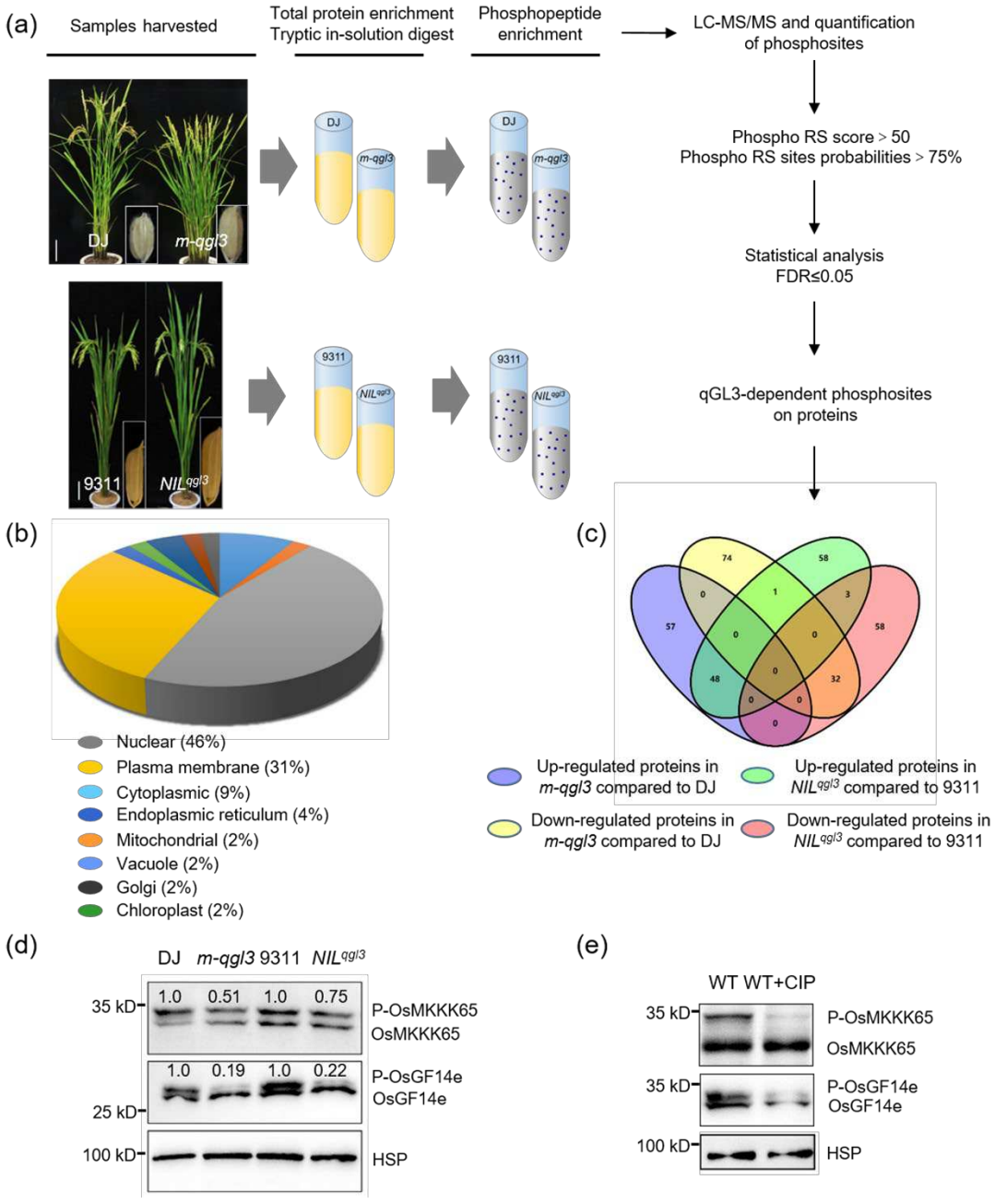

Figure 1. Identification of qGL3-dependent phosphoproteins by quantitative phosphoproteomics.
(a) Schematic representation of the large-scale phosphoscreen individual steps are highlighted and annotated. (b) The subcellular localization of qGL3-dependent phosphoproteins predicted by GO annotation. (c) The number of identified differentially expressed phosphoproteins shown by Venn diagram in DJ, *m-qgl3*, 9311, and *NIL*^{qgl3}. (d) The protein level and status of OsMKKK65 and OsGF14e in DJ, *m-qgl3*, 9311, and *NIL*^{qgl3} plants. For the quantitation of protein level, we first normalized to heat shock protein (HSP), and then analyzed the protein level with the phosphorylated protein level versus the unphosphorylated protein level. The phosphorylated protein level versus the unphosphorylated protein level of DJ or 9311 was defined as 1. (e) Immunoprecipitated OsMKKK65 and OsGF14e proteins from WT was treated with calf intestine alkaline phosphatase (CIP).

This article is protected by copyright. All rights reserved

Accepted Article

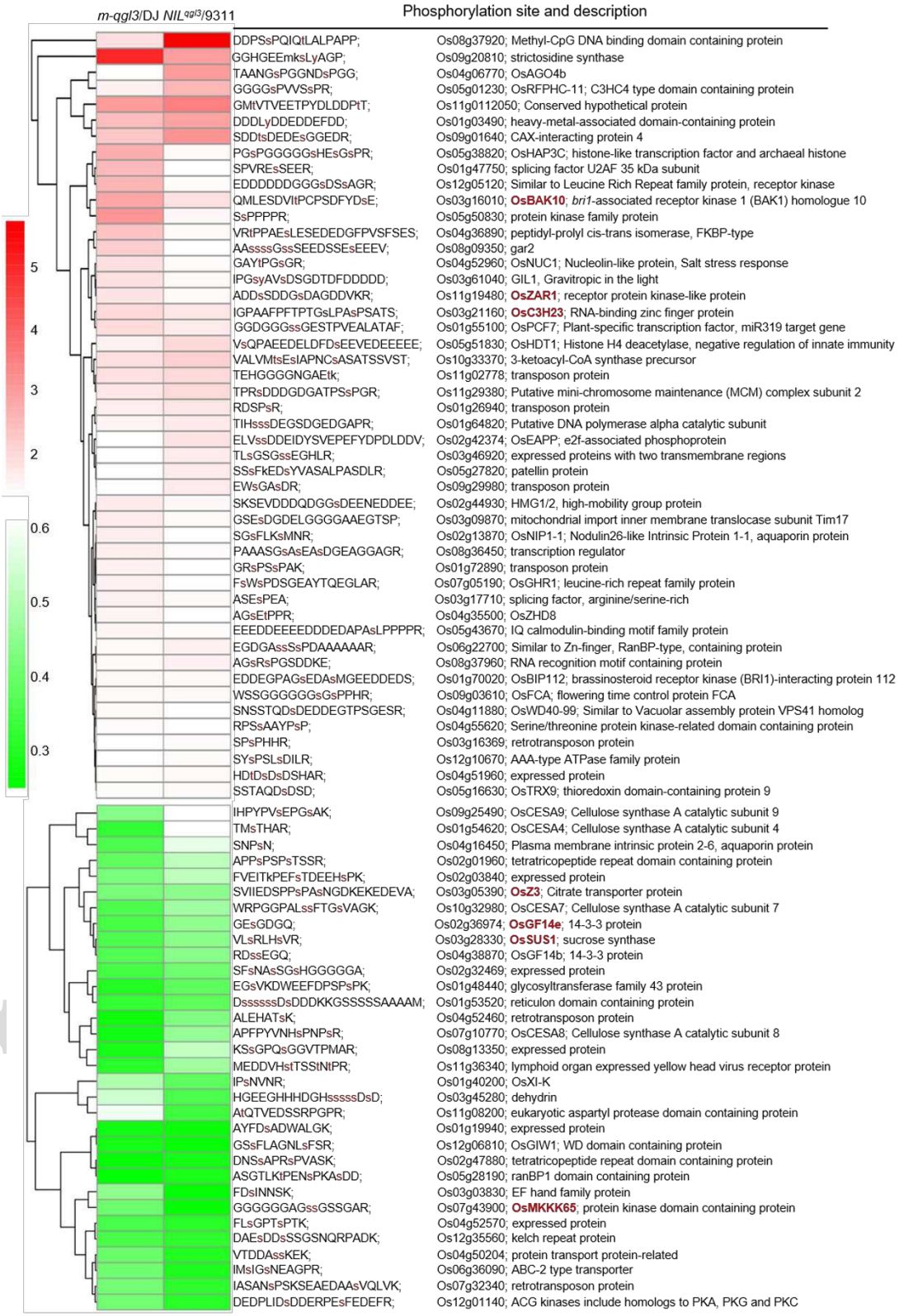

Figure 2. The qGL3-related phosphoproteins commonly detected in two pairs of rice materials (*m-qgl3*/DJ) and (*NIL*^{qgl3}/9311). Hierarchical cluster analysis of the qGL3-dependent phosphosites. For clustering, average estimated phosphosite intensities were normalized per row by median subtraction and colored according to the indicated color gradient. Specific clusters embedding, respectively, upregulated or downregulated phosphopeptides upon (*m-qgl3* vs. DJ) vs. (*NIL*^{qgl3} vs.9311).

This article is protected by copyright. All rights reserved

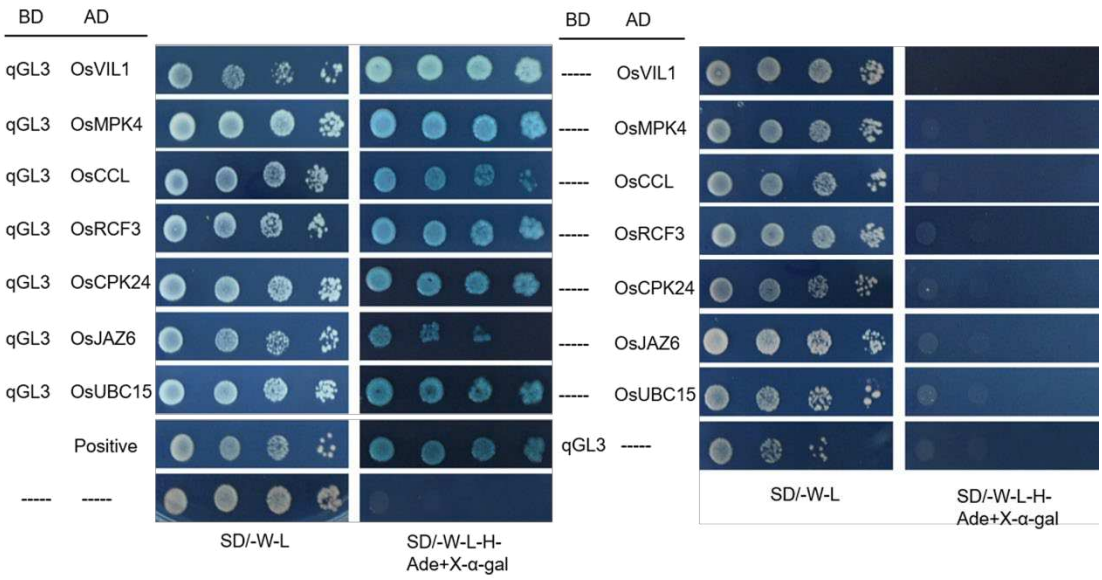

Figure 3. Yeast two-hybrid analysis of qGL3 and its interacting proteins (GIPs). The GIPs were fished from rice young panicle library using qGL3 as bait, including *O. sativa* VERNALIZATION INSENSITIVE3-LIKE1 (OsVIL1), *O. sativa* MAPK4 (OsMPK4), *O. sativa* CYTOCHROME C LIKE (OsCCL), *O. sativa* RNA-binding KH domain-containing protein RCF3 (OsRCF3), *O. sativa* CALCIUM-DEPENDENT PTOTEIN KINASE24 (OsCPK24), *O. sativa* JASMONATE ZIM-DOMAIN PROTEIN6 (OsJAZ6), and *O. sativa* UBIQUITIN CONJUGATING ENZYME15 (OsUBC15).

Accepted Article

This article is protected by copyright. All rights reserved

Accepted Article

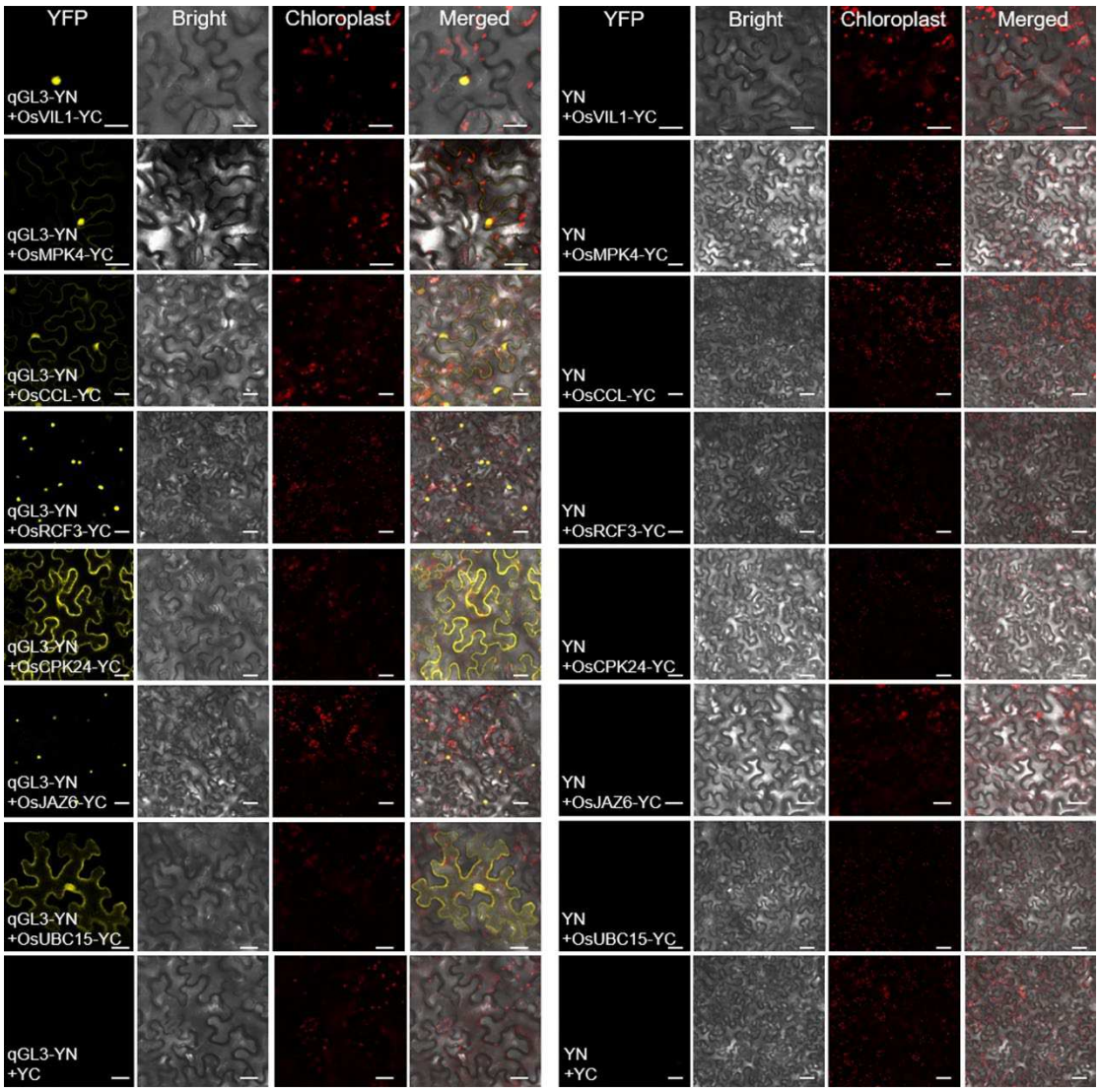

Figure 4. BiFC analysis of the qGL3 and its interacting proteins. The YFP fluorescence signals and autofluorescence signals from tobacco cells were pseudo-colored as yellow and red, respectively. Scale bars, 20 μm.

This article is protected by copyright. All rights reserved

Accepted Article

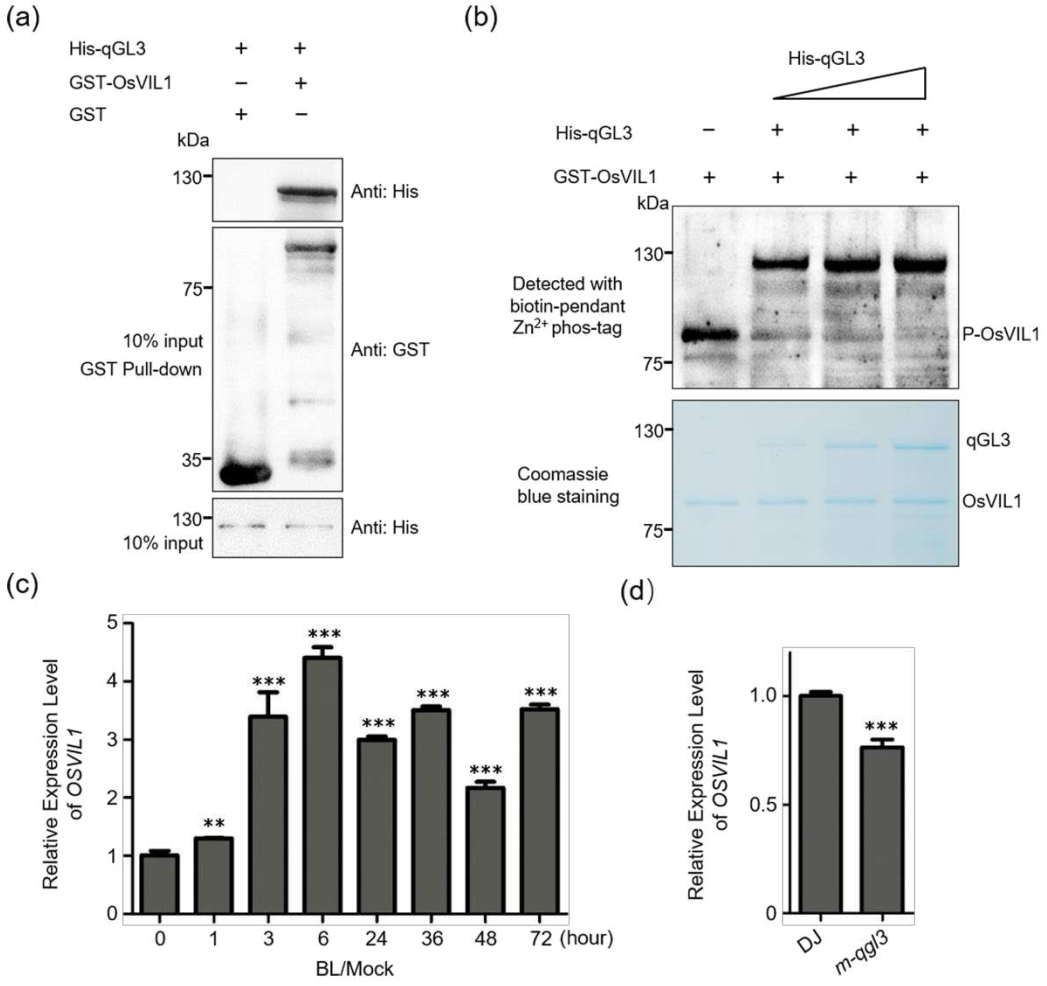

Figure 5. qGL3 interacts with and dephosphorylates OsVIL1.

(a) GST pull-down assay of the qGL3 and OsVIL1 interaction. Anti-His antibody was used to detect the output protein. (b) *In vitro* dephosphorylation analysis. Phosphorylation was detected with biotin-pendant Zn^{2+} phos-tag (BTL-111). Coomassie blue staining of the proteins used for the dephosphorylation assay. (c) The relative expression level of *OsVIL1* under BL treatment. The transcript level of the WT was defined as "1". Data are means ± SE (n = 3). The data were compared by Student's t-test. ***P < 0.001, **P < 0.01. (d) Expression patterns of *OsVIL1* in the seedlings of the WT and *m-qgl3* plants. The transcript level of the WT was defined as "1". Data are means ± SE (n = 3). The data were compared by Student's t-test. ***P < 0.001.

This article is protected by copyright. All rights reserved

Accepted Article

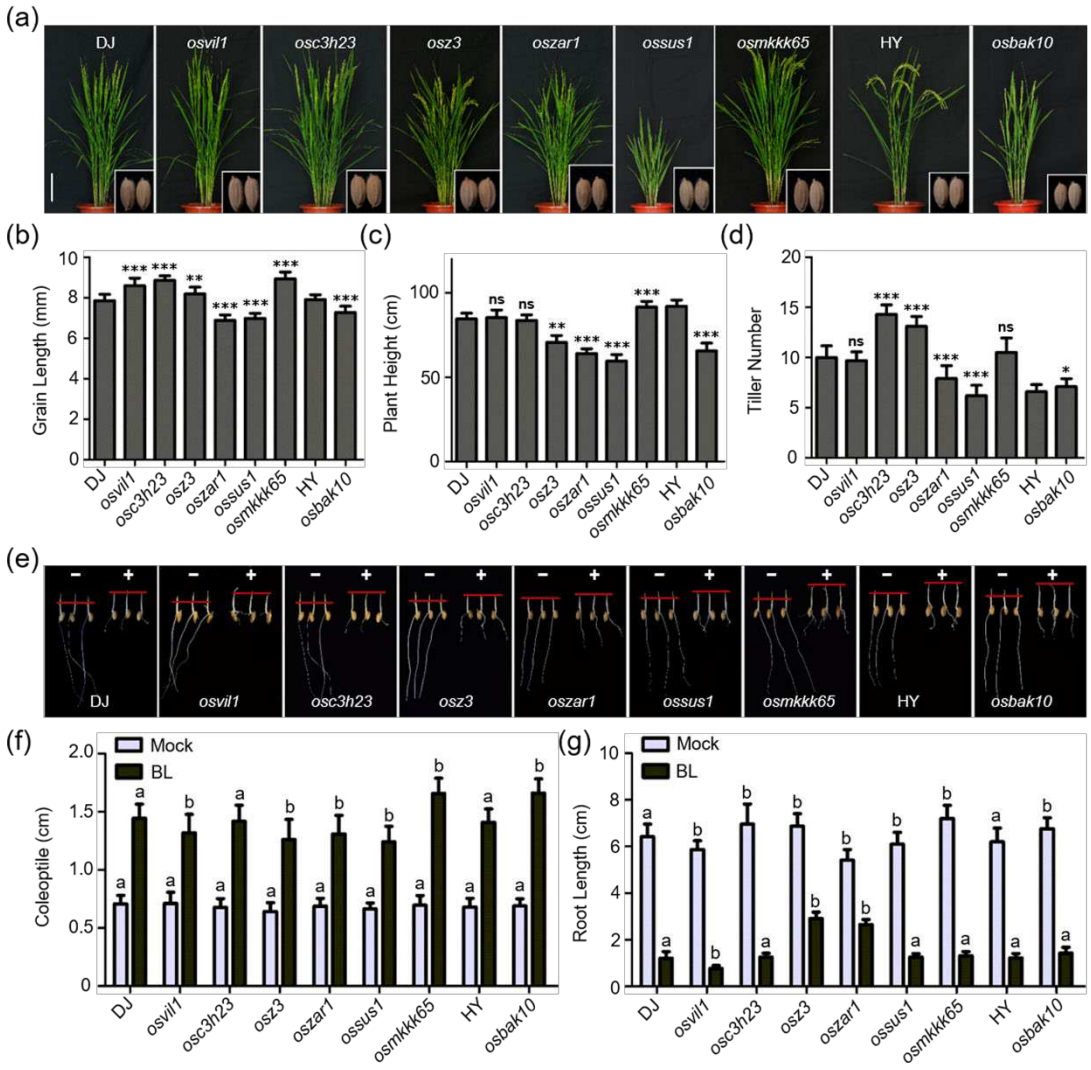

Figure 6. Phenotypes of the mutants of qGL3/OsPPKL1-related proteins.

(a) Morphology of these mutants at the reproductive phase. (b-d) Quantification of grain length (b), plant height (c), and tiller number (d) of these mutants compared with the wild types (Dongjin, DJ; Hwayoung, HY). For quantification of grain length, data are means ± SE (*n* = 15). For quantification of plant height and tiller number, data are means ± SE (*n* = 10). The data were compared by Student's *t*-test. ***P < 0.001, **P < 0.01, *P < 0.05, and "ns" means no significance. (e) Coleoptile elongation and root elongation of the wild types and T-DNA insertion mutant plants in response to 1 μM BL. (f) and (g) Quantitative comparison of coleoptile elongation (f) and root inhibition (g) of these plants. Data are means ± SE (*n* = 15). Statistical analyses were performed by Duncan's multiple range tests. The presence of the same lowercase letter denotes a non-significant difference between wild types and T-DNA insertion mutants under mock or BL treatment, respectively (P > 0.05).

This article is protected by copyright. All rights reserved

Accepted Article

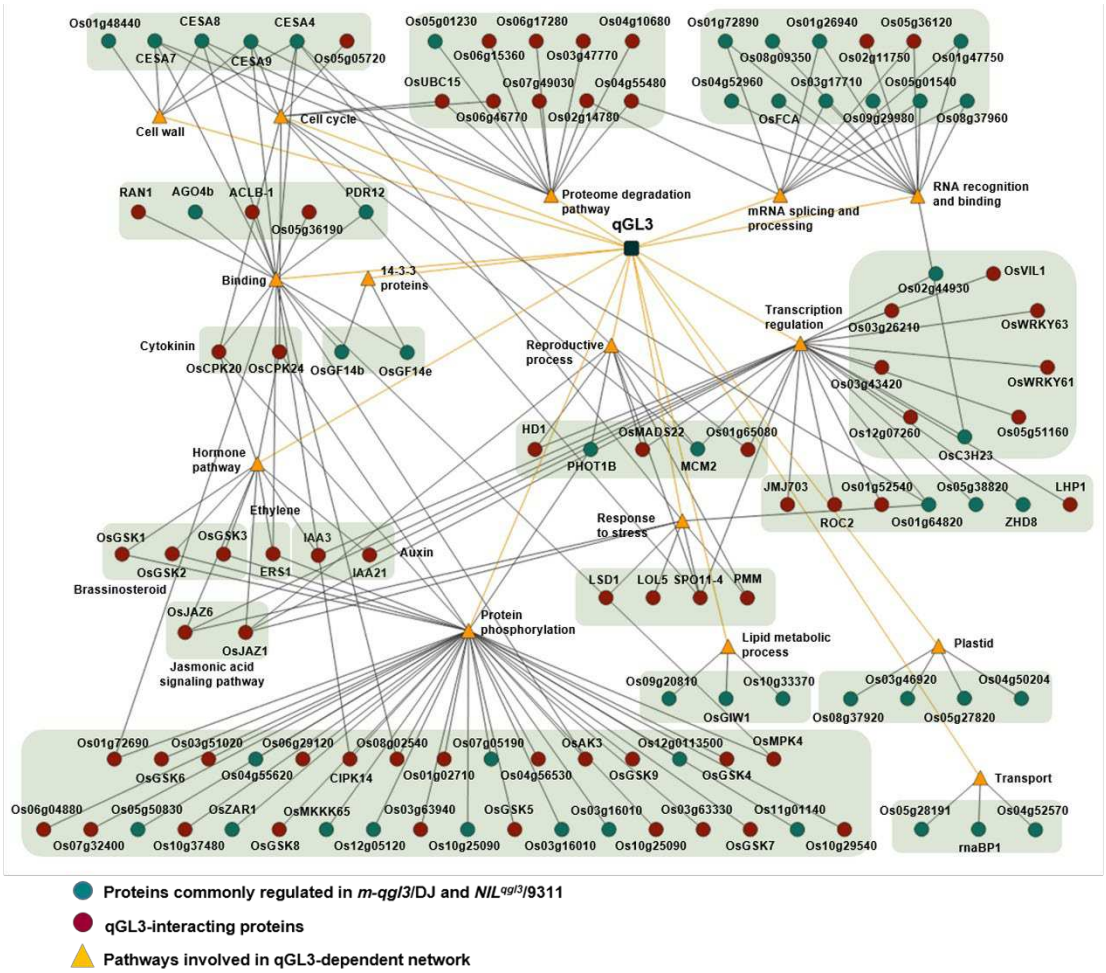

Figure 7. The qGL3-dependent network. For interaction analysis of the qGL3-related phosphorylated proteins and qGL3-interacting proteins, the sequences of the corresponding genes were loaded into String 11.0 (Search Tool for the Retrieval of Interacting Genes/Proteins) (https://string-db.org/) and Cytoscape (version 3.7.2) (http://www.cytoscape.org/).

This article is protected by copyright. All rights reserved